# PREPARATION, CHARACTERIZATION AND CATALYTIC APPLICATIONS OF $MoO_3$ CLUSTERS DISPERSED ON $ZrO_2$

A **Dissertation**
Submitted in partial fulfillment

**FOR THE DEGREE OF**

MASTER OF SCIENCE IN CHEMISTRY

Under The Academic Autonomy

**NATIONAL INSTITUTE OF TECHNOLOGY, ROURKELA**

By

Aparajita Dash

Under the Guidance of

Dr. B. G. Mishra

DEPARTMENT OF CHEMISTRY
**NATIONAL INSTITUTE OF TECHNOLOGY**
**ROURKELA – 769008**
**ORISSA**

# CERTIFICATE

*Dr. Braja Gopal Mishra*
Assistant Professor
Dept. of Chemistry

This is to certify that the dissertation entitled "Preparation, Characterization and Catalytic applications of $MoO_3$ clusters dispersed on $ZrO_2$" being submitted by **Aparajita Dash** to the Department of Chemistry, National Institute of Technology, Rourkela, Orissa, for the award of the degree of Master of Science is a record of bonafide research carried out by her under my supervision and guidance. I am satisfied that the dissertation report has reached the standard fulfilling the requirements of the regulations relating to the nature of the degree.

N.I.T. Rourkela.
Date:06.05.09

Dr. Braja Gopal Mishra
**Supervisor**

## Acknowledgements

*I take this opportunity to express my deep appreciations and indebtedness to Dr. Braja Gopal Mishra, Department of Chemistry, National Institute of Technology, Rourkela, Orissa, for all of his invaluable guidance, continuous encouragement and sharing of frustrations as well as enjoyment throughout this course of research work. Indeed, the experience of working under him is one of that I will cherish forever.*

*It is my great pleasure to acknowledge to Prof. R.K. Patel , Head of the Chemistry Department, National Institute Of Technology, Rourkela for providing me the necessary facilities for making this research work a success .*

*I am indebted to all factulty and staff members of Department of Chemistry, N.I.T, Rourkela for their help.*

*I extend my thanks to my laboratory colleague Mr. Satish Samantaray and Ms. Asfa Ali who were working with me with every difficulty, which I have faced and their constant efforts and encouragement was the tremendous sources of inspiration.*

*Finally, I wish to thank all of my friends for making my stay in this institute a memorable experience.*

**Aparajita Dash**

To

**MY PARENTS**

WHO ENCOURAGE ME

TO PROCEED

AT EVERY STEP

AT EVERY MOMENT

THROUGH

MY LIFE .....

TO SOAR HIGHER

# TABLE OF CONTENTS

# 1. INTRODUCTION

## *1.1 General Introduction*

Metals and their oxides dominate the vast panorama of heterogeneous catalysis. Precious metals including Pt, Pd, Rh, Ru and Ni are employed in various catalytic processes such as naphtha reforming, abatement of automobile emissions, hydrogenation of CO and fats [1]. The metals are employed in the form of finely dispersed particles on high surface area, porous, thermally stable metal oxides, zeolites or carbon supports in order to expose large fraction of metal atoms to reactant molecules. The traditional role of a support is to finely disperse and stabilize the active metal particles by inhibiting their agglomeration during high temperature catalytic applications. The support usually remains inert in catalytic process. Another most important class of materials which have been used as heterogeneous catalyst is the metal oxides. Metal oxides generally exhibit both electron and proton transfer abilities and can be used as catalysts in redox as well as acid-base reactions). The redox properties of oxides are exploited in catalytic purification systems for complete oxidation of toxic materials [2, 3]. The oxide systems with inherent redox properties have also been used for selective oxidation of organic compounds and to synthesize important fine chemicals such as aldehyde, acids and nitriles [4, 5]. The surface acid-base properties of oxides have been taken advantage in carrying out selective organic transformations. The redox properties of many oxides are considered to be important exclusively in catalytic oxidation of hydrocarbons. Many metal oxides are useful as supports for precious metals. Among the metal oxides which have been mostly widely used as catalysts and support, the most prominent are silica, alumina and zirconium dioxide. Silica with different pore structure, pore size and surface properties

have been synthesized in the past decade which has unfolded many of its applications in new areas including heterogeneous catalysis [6]. Ziconium dioxide is an important oxide which has been used extensively for heterogeneous catalytic reactions. Application of zirconium dioxide has been quite promising in catalysis and many other areas due to its versatile structural and surface chemical properties as well as good thermal stability [7, 8]. It has been reported as a better catalyst and catalyst support compared to classical materials such as $Al_2O_3$, $SiO_2$ and $TiO_2$ [9]. The modified versions of zirconium dioxide, viz. the sulfated $ZrO_2$, zirconia substituted mixed oxides such as $Ce_xZr_{1-x}O_2$ solid solutions ($0 \leq x \leq 1$), various transition metal stabilized zirconia and hydrous zirconium oxide have been reported to be effective for several organic reactions, combustion and gas phase reactions [9, 10]. The partial substitution of $ZrO_2$ into $CeO_2$ improves the thermal stability, oxygen storage capacity and redox properties of ceria considerably. This is considered as a significant contribution to three-way catalyst (TWC) technology [10]. However, the role of $ZrO_2$ in $CeO_2$-$ZrO_2$ mixed oxide catalysts seems to be elusive. The catalytic activity of $ZrO_2$ as a single oxide is attributed to the bi-functional acid-base properties, the oxidizing and reducing properties and the terminal and bridged surface OH groups. The catalytic performance of zirconium dioxide depends also on the structural, textural properties, surface area, synthesis method adopted and calcination temperatures .

### *1.2 Structure properties and phase transformation of $ZrO_2$*

$ZrO_2$ is a high temperature ceramic oxide. Its physical properties include high melting point ($2710^oC$) and is resistant to chemical attack by strong acids. Zirconia is also stable

in oxidizing environments, allows oxygen diffusion through its bulk, exhibits good thermal conductivity, and is electrically insulating. These properties enable zirconia to be used as an abrasive, as a hard resistant coating for cutting tools, in oxygen electrodes and sensors, and in high temperature engine components. Structurally, zirconia exists in three polymorphic forms [11, 12]. The high temperature stable form is cubic and possesses a fluorite structure. The Fluorite structure of Zirconia is shown in Figure 1.

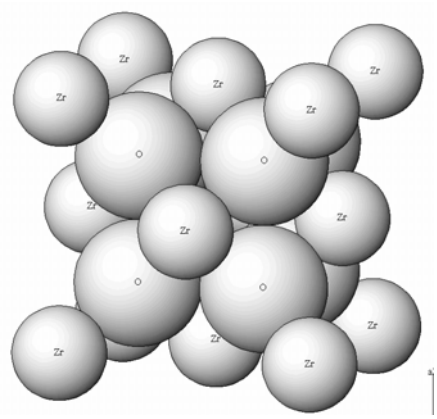


**Figure 1. The hard sphere model for the fluorite structure of $ZrO_2$.**

The structure of $ZrO_2$ can be described as the $Zr^{4+}$ ions forming a cubic close pack structure (FCC lattice) with the $O^{2-}$ ions occupying all the tetrahedral holes. In the FCC structure, the $Zr^{4+}$ ions occupy all the corners and the face center position of the cube. If the cube is divided into eight symmetric smaller cubes through its centre, then the oxygen ions occupy the centers of all the smaller cubes (figure 2).

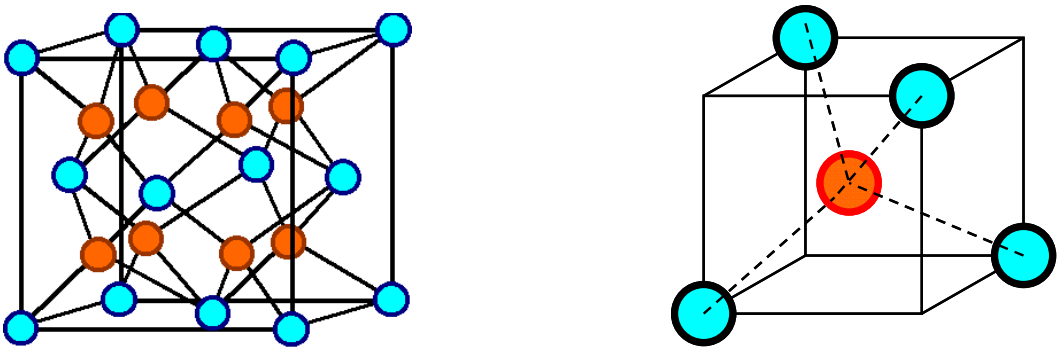

(a) (b)

**Figure 2. (a) The fluorite structure of $ZrO_2$ and (b) The tetrahedral sites (Red Dot: $O^{2-}$ and cyan dot: $Zr^{4+}$)**

The fluorite structure of $ZrO_2$ can be described in an alternate way where the $Zr^{4+}$ ions are present in the centre of the cube with $O^{2-}$ ions are present at the corner of the cube. Half of such cube centers are vacant where as half of them are occupied by $Zr^{4+}$ ions. One unit cell of $ZrO_2$ consists of eight such cubes (Figure 3).

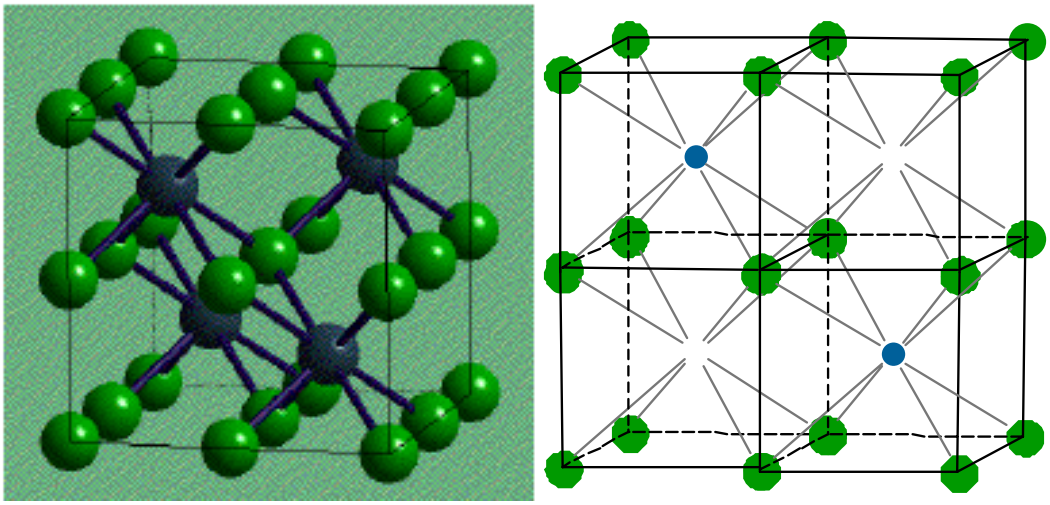

**Figure 3 The fluorite structure of $ZrO_2$ (Green Dot: $O^{2-}$ and blue dot: $Zr^{4+}$)**

With decreasing temperature, $ZrO_2$ undergoes a cubic to tetragonal ($c \rightarrow t$) phase transition at around 2380°C and a tetragonal to monoclinic ($t \rightarrow m$) phase transition at around 1205°C[11, 12]. At the cubic to tetragonal phase transition, the fluorite cubic structure

distorts to the tetragonal structure with the tetragonal *c*-axis parallel to one cubic <001> axes. The characteristics of this phase transition are (i) displacement of oxygen ions from the fluorite site, (ii) occurrence of cell doubling, $Z=1$ to $Z=2$, (iii) ferroelastic property in the tetragonal phase, and (iv) lower shift of the phase transition points by incorporating oxygen defects and/or metals ions such as $Y^{3+}$, $Mg^{2+}$, and $Ca^{2+}$.

On the other hand, the tetragonal to monoclinic phase transition is characterized by a martensitic phase transition accompanied by large hysteresis in the phase transition temperature, greater than 200°C, and the generation of large shear and volume elastic strains in the monoclinic phase [11, 12]. The tetragonal to monoclinic phase transformation is governed by the free-energy change of the entire system, $\Delta G_{t\rightarrow m}$, which depends on the chemical free-energy change, $\Delta G$c, the strain energy change, $\Delta U_{se}$ and the energy change associated with the surface of the inclusion $\Delta U_s$, The net free energy change is given by .

$$\Delta G_{t\rightarrow m} = -|\Delta G_c| + \Delta U_{se} + \Delta U_s$$

It has been observed that the martensitic transformation temperature for the $t\rightarrow m$ can be brought down significantly by adding additives of suitable characteristics which facilitates the stabilization of the tetragonal phase. The monoclinic and tetragonal unit cell of $ZrO_2$ is shown schematically in figure 4.

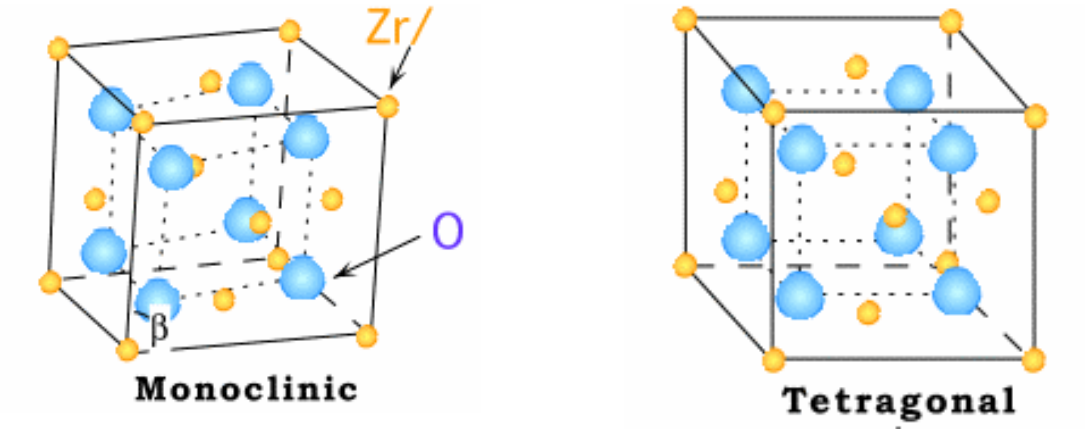


**Figure 4. The monoclinic and tetragonal unit cell of $ZrO_2$**

### *1.3 Importance of $ZrO_2$ based materials in catalysis*

As discussed earlier, $ZrO_2$ is an amphoteric oxide which displays surface acid-base properties. The acid-base properties of $ZrO_2$ have been exploited to carry out many organic reactions on its surface including, dehydration, hydrogen transfer reaction and Friedel Craft alkylation reactions. In addition to its application in industrial applications $ZrO_2$ has many technological applications as catalyst and promoter in environmental catalytic processes and energy devices. The following is a brief account for application of zirconia as catalyst.

#### *1.3.1 Zirconia as a promoter in three way catalyst*

The three important pollutants present in automobile exhaust are (i) uncombusted hydrocarbons (HC), (ii) carbon monoxide (CO) and (iii) nitrogen oxides ($NO_x$). The three-way catalyst (TWC) converts these three pollutants to environmentally acceptable carbon dioxide, water and nitrogen. The commercially employed TWC formulation contains Pt/Pd, Pt/Pd/Rh, Pd-only and Pd/Rh noble metal catalysts [13]. The concentrations of these pollutants in the exhaust depend on the air-fuel ratio (A/F) in the

combustion chamber. If the air-fuel ratio is close to the stoichiometric value of 14.6, the catalyst converts all the pollutants to $CO_2$, $H_2O$ and $N_2$ gases with high efficiency. The conversion efficiency plot for HC, CO and $NO_x$ as a function of air-fuel ratio is given in Fig. 5. The plot shows the highest conversion of pollutants at the stoichiometric value. Ceria and ceria-based oxides also incorporated in the TWC formulation. The role of ceria in TWC is to widen the A/F window and help maintaining the conversion efficiency of the catalyst. Ceria can absorb oxygen under lean fuel conditions and release oxygen during fuel rich conditions. This happens because of its ability to switch between $Ce^{4+}$ and $Ce^{3+}$ oxidation states depending on the oxygen partial pressure in the exhaust.

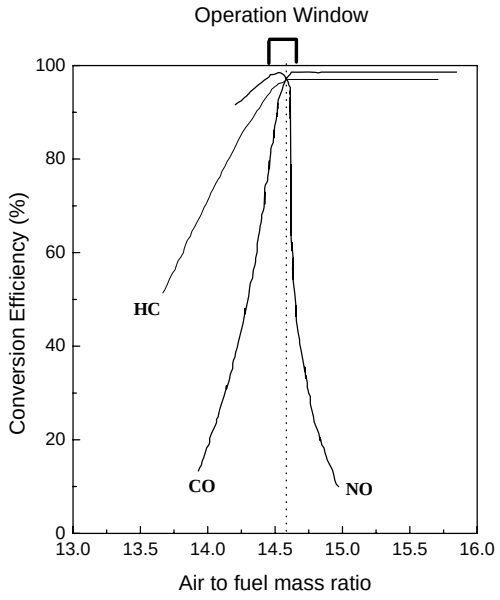


**Figure 5.Effect of air to fuel ratio on the conversion efficiency of three-way catalyst**

While using ceria based materials in important catalytic processes such as three way catalysis, the major concern is the thermal stability of the ceria component at higher temperatures. For example, to increase the efficiency of TWCS during a cold start,

closed-couples locations of the converter are usually employed. Therefore, in the driving condition the operating temperature exceeds 1200K. At such higher temperature the deactivation of the catalyst may occur due to sintering of metal particles. In addition to that the oxygen storage capacity of ceria strongly decreases upon thermal aging due to the growth of ceria crystallite, loss in active surface area and /or formation of $CeAlO_3$ phases. The thermal stability and redox behavior of ceria can be improved by incorporation of zirconia into the cubic lattice of ceria [15-17]. Ceria is known to form a substitutional type solid solution with zirconia [15]. The ceria-zirconia solid solutions show better oxygen storage capacity and reduction behavior compared to pure ceria and is regarded as a potential substitute for ceria in TWC applications [15, 16]. Ceria-zirconia solid solution exists in three different phases namely monoclinic, tetragonal and cubic. The cubic and monoclinic phases are thermally stable below 1300K, where as the tetragonal phase is a metastable phase and can be prepared by high temperature ceramic method in the composition range of 10-50 mol% of ceria [16]. Above 50 mol% of ceria, the cubic phase is formed. The kinetics of the redox process is favored in the cubic phase compared to the tetragonal and monoclinic phases [16]. The TPR profile of ceria is modified to a large extent upon incorporation of zirconia into the ceria lattice. Figure 4 shows the TPR profile of three high surface area $CeO_2$-$ZrO_2$ solid solutions compared with the TPR profile of pure ceria. The oxide solid solutions undergo reduction in the region between 500 K and 950 K with different $T_{max}$ values.

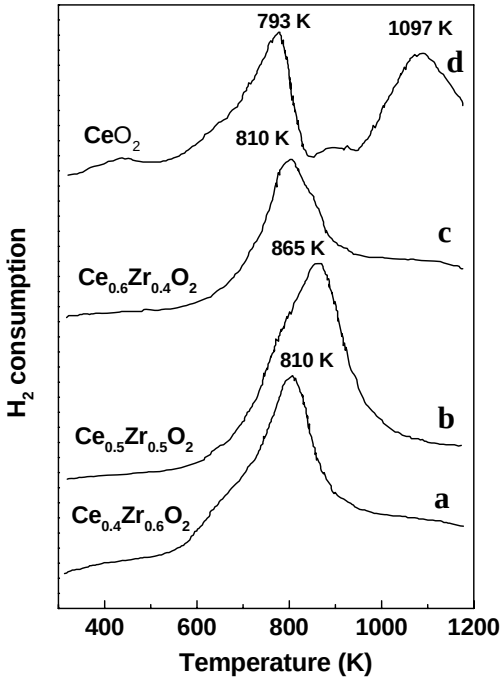


**Figure 6.** TPR profiles of $CeO_2$-$ZrO_2$ solid solutions in comparison to that of $CeO_2$

Two important aspects to be noticed from the figure 5 is that (i) The solid solutions undergo maximum reduction at temperatures close to the surface reduction of pure ceria and (ii) The surface and bulk reduction signatures, observed for pure ceria, are merged together in the solid solutions. This suggests that the whole ceria components including the bulk part, in the solid solution is subjected to reduction in a single stage. This change in reduction feature has been explained in terms of facile migration of oxygen ions in the $CeO_2$-$ZrO_2$ lattice [17].

### *1.3.2 Solid oxide fuel cells*

Solid oxide fuel cell is an energy device which is a possible source of non-conventional energies and clean alternative to fossil fuels. Fuel cells efficiently convert chemical energy to electricity an environmentally friendly way. They are a promising alternative to traditional mobile and stationary power sources, such as the internal combustion engine

and coal burning power plants. Among the various kinds of fuel cells, solid-oxide fuel cells (SOFCs) have the advantages of the highest energy conversion efficiency and excellent fuel flexibility because of their high operating temperature [18]. Although the concept of SOFCs was developed more than a century ago, they have never received such considerable attention as in the past decades, due to the increasing attention for a sustainable development. Fig. 7 illustrates the operating principles for an SOFC. The typical SOFC single cell consists of three main components, i.e., a porous cathode (or air electrode) and a porous anode (or fuel electrode), sandwiching a dense electrolyte. The distinguishing feature of SOFCs is that the electrolyte is an electronic insulating ion conducting ceramic that allows only the proton or oxygen ion to pass through. The cathode functions as the electrocatalyst for reduction of oxygen into oxide ions. When an oxygen ionic conducting oxide is adopted as the electrolyte, these ions then diffuse through the solid-oxide electrolyte to the anode, where they electrochemically oxidize the fuel. The released electrons flow through an external circuit to the cathode to complete the circuit and to do work. The most important component of the SOFC is the ceramic electrolyte. The yttria-stabilized zirconia (YSZ) is used as an efficient electrolyte in SOFC. The presence of $Y_2O_3$ in the Zirconia matrix is found to stabilize the cubic phase of zirconia and helps in the ionic conductance [19].

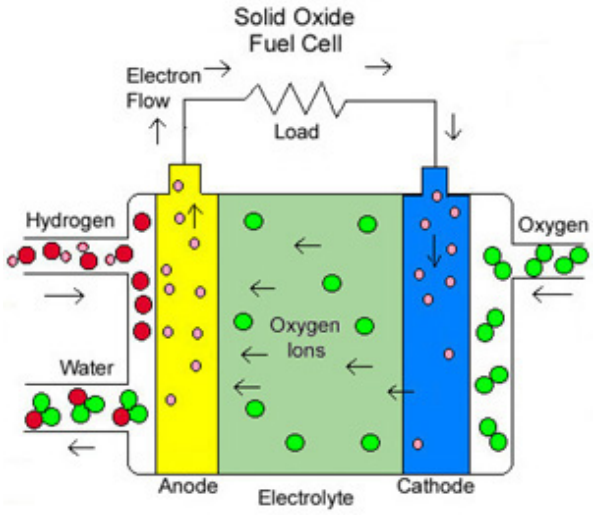


Figure 7. Schematic representation of a Solid oxide fuel cell

### *1.3.3 Anchoring of $WO_3$, $SO_4^{2-}$ and $MoO_3$ on $ZrO_2$ surface*

Although $ZrO_2$ has been used as an acid-base catalyst for numerous organic reactions in heterogeneous catalysis, its application has however been limited by the presence of mild acidic and basic sites on its surface. In this regard recent years, there are many investigations on increasing the surface acid strength of zirconia by surface modification. The most prominent among them is anchoring catalytically active metal oxides and anions such as $WO_3$, $SO_4^{2-}$ and $MoO_3$ at submonolayer level to generate newer acidic sites. The results achieved in recent years are quite remarkable considering the fact that strength of the order of 100% $H_2SO_4$ can be achieved by these modifications which is rarely found in any heterogeneous catalyst. The grafting of sulfated species on ZrO2 strong acidic sites on their surfaces often termed as “superacidic” which are capable of catalyzing carbonium ion reactions under mild conditions. The relatively simple method of preparation of these catalysts makes them one of the attractive classes of heterogeneous catalysts. Sulfated metal oxides can be prepared by treatment of the host oxides with sulfuric acids or ammonium sulfate solutions [20]. Acid treatment of the

hydrous form of the metal oxides has been reported to produce catalysts with better physicochemical properties. The hydrous form of the metal oxides can be prepared by heat treatment of hydroxide precursors of the metal ions at lower temperature in the range of 300-500$^{o}$C. There have been numerous investigations on the acidic properties of sulfated metal oxides using TPD, FTIR of adsorbed probe molecules and NMR spectroscopy. Generation of acidic sites on sulfated oxides, thought to proceed by a two stage reaction mechanism involving grafting of the sulfate species during impregnation step followed its dehydration at higher temperatures [6] (shown below).

First step: Impregnation followed by drying

$Zr_n(OH)_{4n} + H_2SO_4 \rightarrow Zr_n(OH)_{4n-2x}(SO_4)_x + 2xH_2O$

Second step: Calcination above 400 $^{o}$C

$Zr_n(OH)_{4n-2x}(SO_4)_x \rightarrow Zr_nO_{2n-x}(SO_4)_x + 2(n-x)H_2O$

The sulfated metal oxides are known to display both Lewis and Bronsted acidic properties. Several surface reaction scheme have been proposed in literature to account for both form of acidity observed in these materials. The most prominent among them are by Arata and Hino [21] (Figure 8) and Clearfield et al. [22] (Figure 9) which takes into account the generation of surface Lewis and Bronsted acidic sites. Sulfated $ZrO_2$ and $SnO_2$ have been used as catalysts for several industrially important chemical reactions such as alcohol dehydration, olefins hydration, esterification, Friedel-Crafts acylation and isomerization reactions.

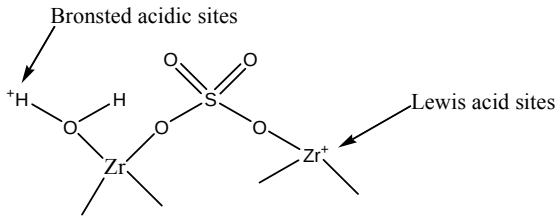


Figure 8. Schematic presentation of the Bronsted and Lewis acidic sites in sulfated zirconia proposed by Arata and Hino

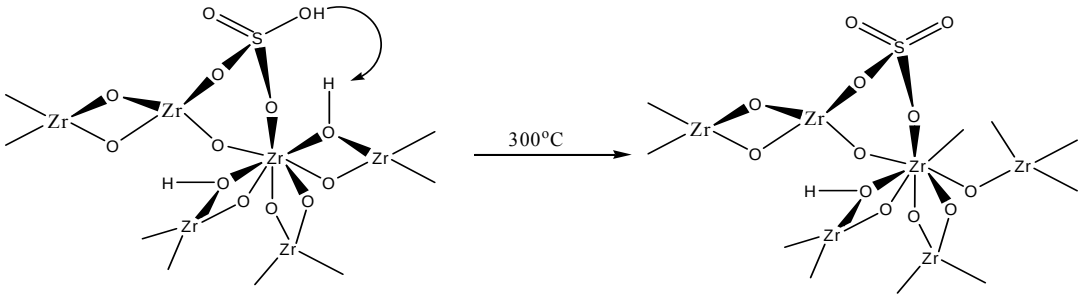


Figure 9. Schematic presentation of the Bronsted and Lewis acidic sites in sulfated zirconia proposed by Clearfield et al.

Tungsten oxide species dispersed on zirconia supports (WO*x*-$ZrO_2$) comprise another interesting class of solid acids [23]. The strong acid sites originates on these materials when zirconia oxyhydroxide ($ZrO_x(OH)_{4-2x}$) is impregnated with solutions containing tungstate anions and then oxidized at high temperatures. The addition of a small amount of platinum (<1 wt % Pt) to preoxidized WO*x*-$ZrO_2$ samples leads to the formation of active, stable, and selective catalysts for *n*-alkane isomerization reactions The Pt/WO*x*-ZrO2 have shown to catalyze efficient hydrogen transfer steps prevent extensive cracking of adsorbed carbocations by limiting their surface lifetimes [24]. Several recent publicaions describe the synthesis and catalytic activity of WO*x*-$ZrO_2$ and Pt/WO*x*- $ZrO_2$ for several hydrocarbon reactions (cyclohexane ringopening and isomerization, benzene hydrogenation, alkene oligomerization, aromatic alkylation with alkenes or methanol, aromatic trans-alkylation, and heteroatom removal) [25].

# CHAPTER 2

# MATERIALS AND METHODS

## *2.1 PREPARATION OF CATALYSTS*

### *2.1.1 Preparation of $MoO_3$-$ZrO_2$ catalysts by pH controlled coprecipitation*

The $MoO_3$(x mol%)-$ZrO_2$ materials of different compositions were prepared by pH controlled precipitation using zirconium oxychloride ($ZrOCl_2.xH_2O$) (S.D. Fine chemicals India Ltd.), ammonium heptamolybdate ($(NH_4)_6Mo_7O_{24}$) and liquid ammonia (S.D. Fine Chemicals India Ltd.) as starting materials. Required amount of zirconyl chloride and ammonium heptamolybdate solution were added dropwise to 200 mL of deionised water whose pH was previously adjusted to 9.5 by addition of liquid ammonia solution. During the addition of metal salt solution, the pH of the mixture was found to decrease due to the hydrolysis of the salts. The pH was maintained at 9.5 by controlled addition of ammonia solution to the reaction mixture. The precipitated solution was stirred for 6 hr at room temperature followed by filtration and washing with double distilled water until free from chlorine ($AgNO_3$ test). The hydroxide precipitate were subsequently dried overnight at 120$^oC$ and calcined at 500 $^oC$ for 2 hr to generate $MoO_3$-$ZrO_2$ catalysts. Using this method, the $MoO_3$(x mol%)-$ZrO_2$ catalyst where x = 2, 5 and 20 were synthesized. These materials are refereed to as xMoZr materials in subsequent discussions.

### *2.1.2 Preparation of $MoO_3$(20 mol%)-$ZrO_2$ catalysts by wet impregnation method*

For the sake of comparison, the $MoO_3$(20 mol%)-$ZrO_2$ catalyst was also prepared by wet impregnation technique. To an 25 ml aqueous suspension of $ZrO_2$, 50 ml of the required amount of ammonium heptamolydate solution was added and stirred for 12 h. The

aqueous suspension was then heated under stirring to remove the water. The obtained material was subsequently dried overnight at 120 $^{o}$C and calcined at 500 $^{o}$C for 2 hr to generate $MoO_3$(20 mol%)-$ZrO_2$ catalysts. This material is refereed to as 20MoZrC catalyst in the subsequent discussion.

## 2.2 CHARACTERIZATION OF CATALYST MATERIALS

The synthesized materials in section 2.1 were characterized by X-Ray diffraction, Scanning Electron Micrograph and Raman Spectroscopy.

### X-ray diffraction

The X-ray diffraction patterns of the xMOZr and 20MoZrC samples were recorded on a Siemens D-500 diffractometer using Ni-filtered $CuK_\alpha$ radiation. The XRD measurements were carried out in the 2θ range of 20-70$^{o}$ with a scan speed of 2 degrees per minute using Bragg-Brantano configuration.

### Scanning Electron Micrograph

Scanning electron microscopy pictures were taken using JEOL JSM-5300 microscope (acceleration voltage15 kV). The sample powders were deposited on a carbon tape before mounting on a sample holder for SEm analysis.

### Raman Spectroscopy

The Raman spectra were recorded with a LabRam spectrometer (Dilor) equipped with a confocal microscope (Olympus) and a He–Ne laser. The slit width was usually set to 200 μm resulting together with the used 1800 grating in a spectral resolution of 2 $cm^{-1}$. For conventional Raman spectroscopy, the laser power of the He Ne laser attached to the LabRam spectrometer was set at 0.14 mW by neutral density filters.

### *2.3 Synthesis of β-acetamidoketones*

To a solution of the arylaldehyde (2 mmol), aryl ketone (2 mmol), acetyl chloride (4 mmol) in acetonitrile (4 ml) was added 100 mg of 20MoZr catalyst and heated at 50$^{o}$C, with stirring for the required amount of time. The progress of the reaction was followed by TLC on 0.2 mm silica gel F-254 plates. After completion of the reaction, the 20MoZr catalyst was filtered and the filtrate was poured into 50 ml ice-water. The ensuing solid product was filtered, washed with ice-water and recrystallized from ethylacetate/n-heptane to give the pure product. The products were characterized by comparison of their melting points and IR spectroscopic data with that of literature reported values. Melting points were measured on a Micro Scientific Works apparatus and are uncorrected. The IR spectra of different samples (as KBr pellets) were recorded using a Perkin-Elmer infrared spectrometer with a resolution of 4 $cm^{-1}$, in the range of 400 $cm^{-1}$ to 4000 $cm^{-1}$. Nearly 3-4 mg of the sample was mixed thoroughly with 30 mg of oven dried KBr and made into pallets. The pallets were stored in vacuum desiccators. Prior to the IR measurement, the background correction was performed using pure KBr pallets.

## 3. RESULT AND DISCUSSION

### *3.1 X-ray diffraction study*

Figure 1 shows the X-ray diffraction patterns of the xMOZr catalysts along with the pure $ZrO_2$ and 20MoZrC catalyst. The pure $ZrO_2$ catalyst prepared by the precipitation method shows intense and well defined diffraction peaks at 2θ values of 28.1, 31.4, 34.1, 40.9 and 50.2 degrees corresponding to the d values of 3.17 Å, 2.84 Å, 2.62 Å, 2.2 Å and 1.8 Å, respectively. These peaks are characteristics of the presence of the monoclinic phase of $ZrO_2$. Adding 2 mol% Mo into the $ZrO_2$ lattice results in a change in the peak pattern of the host zirconia (Fig. 10B). The peaks corresponding to the monoclinic phase looses intensity simultaneously a new intense peak appear at 2θ value 30.2 degrees corresponding to the d value of 2.95 Å. This peak corresponds to the presence of tetragonal phase in the 2MoZr sample. It was observed that the addition of Mo into the ZrO2 lattice favors the formation of the tetragonal phase selectively. The martensitic transformation temperature has been found to be reduced from 1205$^{o}$C to 500$^{o}$C upon addition of 2% $MoO_3$ into $ZrO_2$. The percentage tetragonal phase present in the mixture was evaluated by using the method proposed by Devassy et al [27]. The 2MoZr sample was found to contain 69% tetragonal phase. Increasing the $MoO_3$ content to 20 mol% further resulted in the change in the XRD patterns. All the characteristics peaks corresponding to the monoclinic phase was found to be absent in the 20MoZr material. The 20MoZr catalyst shows 100% tetragonal phase in the composite material indicating that the presence of $MoO_3$ in $ZrO_2$ matrix facilitates the monoclinic to tetragonal phase transformation. The XRD pattern of the 20MOZrC catalyst prepared by the wet impregnation method is shown in Fig. 1d. Although this material contains equal amount

of $MoO_3$, it is found to contain a substantial amount of monoclinic phase. The 20MOZrC catalyst contains a mixture of monoclinic and tetragonal phases. This observation clearly points to the effect of preparation method on the phase content and properties of the composite catalyst.

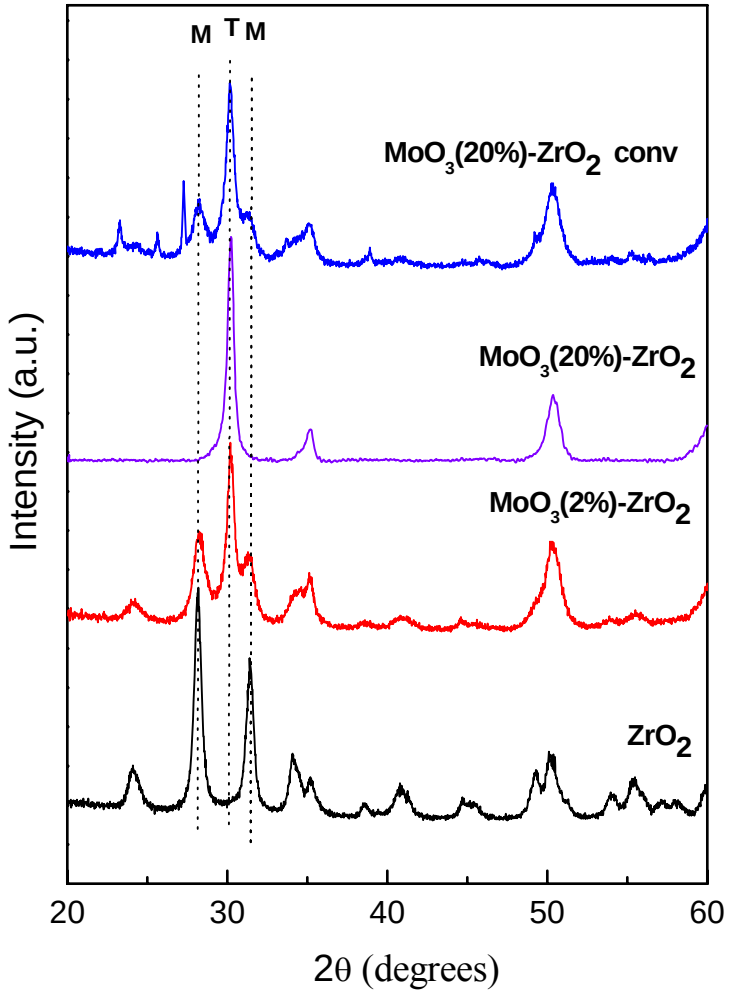


**Figure 10. X-ray diffraction patterns of (a) $ZrO_2$, (b) $MoO_3$(2%)-$ZrO_2$, (c) $MoO_3$(20%)-$ZrO_2$ and (d) $MoO_3$(20%)-$ZrO_2$ conventional catalyst.**

The 20MOZr catalyst prepared by pH controlled hydrolysis contain well dispersed $MoO_3$ particles due to the molecular level mixing of the precursors during hydrolysis, where as

the conventionally prepared catalysts contains segregated particles. Because of the lesser grain boundary area of contact between the $MoO_3$ and $ZrO_2$ particles in the later case the phase transition of $ZrO_2$ is not completely accomplished. The volume average particle size of the composite oxides prepared by ph controlled hydrolysis is calculated by using the Scherrer's equation which is found to be in the range of 10-20 nm.

### *3.2 SEM study*

The scanning electron micrograph of the 20MoZr catalyst is shown in figure 2. The $MOO_3$(20%)-$ZrO_2$ composite particles are of irregular shape and size with good dispersion of the component oxides.

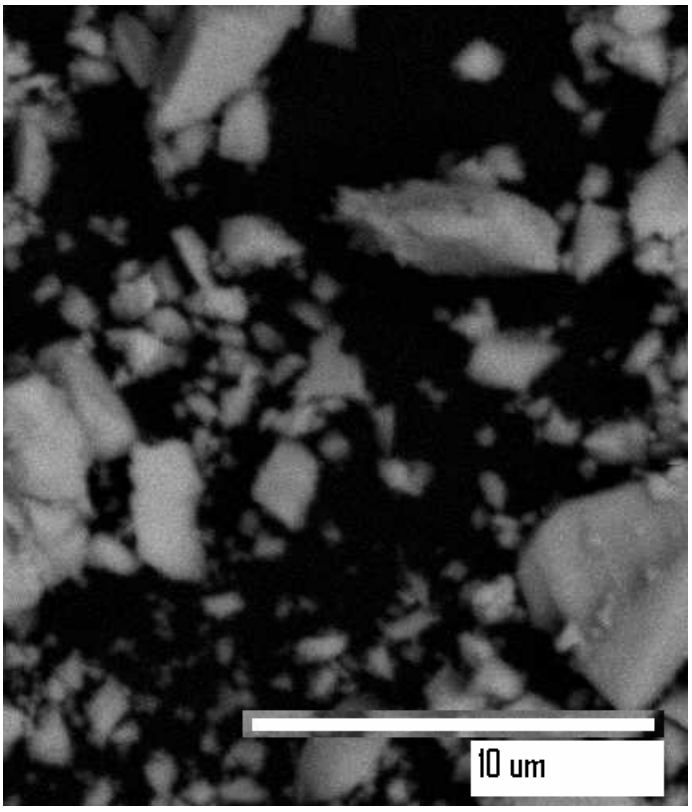


Figure 2. Scanning Electron Micrograph of 20MoZr catalyst.

### *3.3 Raman Spectroscopic study*

The Raman spectra of the 2MoZr, 20MoZr along with the pure $MoO_3$ catalyst in the range of 700-1200 $cm^{-1}$ is shown in figure 3. Since, pure $ZrO_2$ strongly absorbs infrared radiation below 700 $cm^{-1}$ and hence mask the absorption of the $MoO_3$, the absorption data below 700$cm^{-1}$ are not collected in the present study.

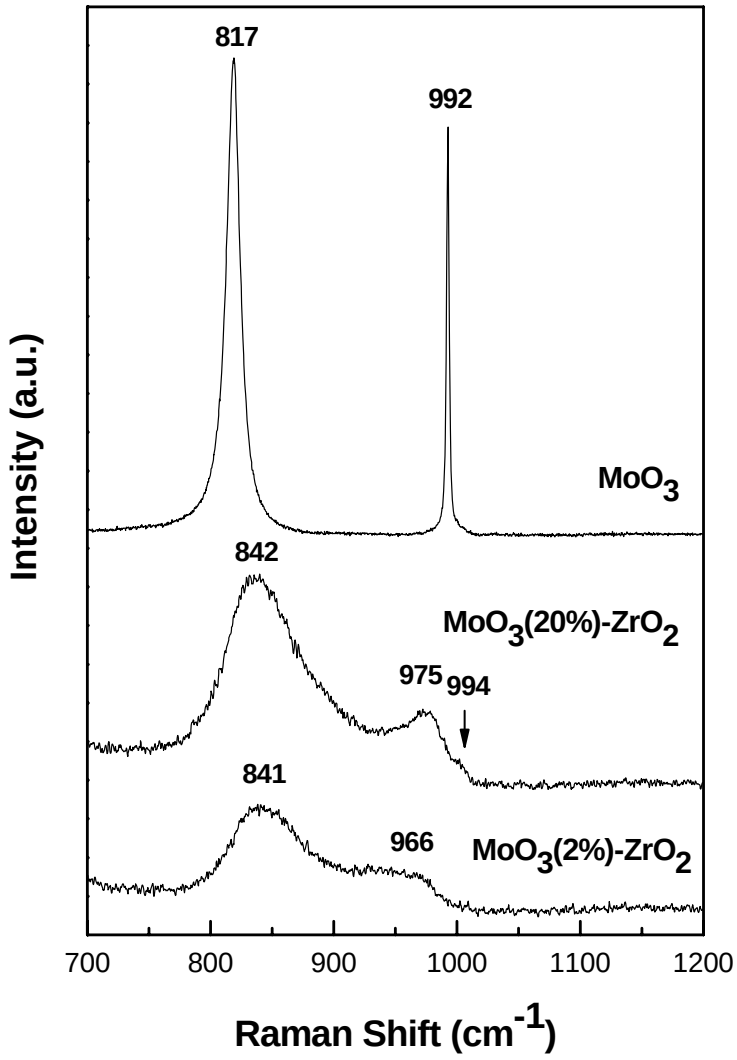


**Figure 3. Raman spectra of (a) $MoO_3$, (b) $MoO_3$(20%)-$ZrO_2$ and (c) $MoO_3$(20%)-$ZrO_2$ catalyst**

Pure $MoO_3$ shows two intense and well defined absorption peaks at 817 and 992 $cm^{-1}$ corresponding to the presence of highly polymerized $MoO_3$ species in the sample. When 2% $MoO_3$ was dispersed in the $ZrO_2$ matrix, the peak pattern observed was completely different than the pure $MoO_3$. The 2MOZr catalyst, shows two broad peaks at 842 and 966 $cm^{-1}$. The peak at 842 $cm^{-1}$ have been assigned to the terminal M=O vibration of isolated $MoO_4^{2-}$ species where as the broad and low intensity peak at 966 $cm^{-1}$ peak has been assigned to the asymmetric stretching Mo-O-Mo vibration similar to the $Mo_7O_{24}^{6-}$ and $Mo_8O_{26}^{6-}$ species [28, 29]. These peak positions were found to change and shift toward higher side with increase in the $MoO_3$ content. These peak positions were observed at 842 and 975 $cm^{-1}$ respectively for the 20 MoZr catalyst. In addition, the 20MoZr catalyst shows a additional small shoulder at 994 $cm^{-1}$ which is identical to that of the polymerized $MoO_3$ species. The raman study clearly indicate the presence of different type of molecular $MoO_3$ species on $ZrO_2$ surface depending upon the $MoO_3$ content. At low $MoO_3$ loading, isolated unimolecular $MoO_4^{2-}$ species is present on the $ZrO_2$ surface along with the $Mo_7O_{24}^{6-}$ and $Mo_8O_{26}^{6-}$ clusters, whereas with increase in loading the bulk type characteristics of the $MoO_3$ is prevailed in the composite oxide sample. The presence of different molecular species on the $ZrO_2$ surface is shown schematically in the figure 4.

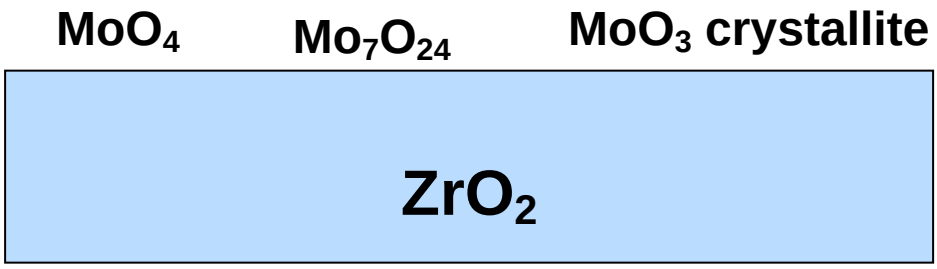


Figure 4. Pictorial representation of the different $MoO_3$ molecular species on $ZrO_2$ surface.

### *3.4 Synthesis of β-acetamidoketones*

Acetamidoketones are a class of organic compounds with interesting biological and pharmacological properties. These compounds are used for preparation of antibiotic drugs such as nikkomycine or neopolyoxines [30]. The synthesis of β-acetamidoketones has been accomplished by the Dakin–West reaction by condensation of α-amino acid with acetic anhydride in the presence of a base [31]. Recently, improved synthetic routes have been developed for the synthesis of β-acetamido ketones involving the acid catalyzed multicomponent condensation reaction of aryl aldehydes, enolizable ketones, acetyl chlorides and acetonitrile. Several Lewis and Bronsted acids such as $CoCl_2$, heteropoly acids, $BiCl_3$ generated from BiOCl, $Sc(OTf)_3$ and $ZrOCl_2.8H_2O$ have been used as catalysts under homogeneous condition for the synthesis of β-acetamidoketones [32]. However, due to the inherent disadvantages of separation and recyclability associated with the homogeneous catalysts there has been afford to develop heterogeneous catalytic route for the synthesis of these biologically important class of compounds. The heterogeneous catalysts used for this multicomponent condensation reaction include among others sulfuric acid absorbed on silica, montmorillonite K-10 clay and ZnO [33]. However, the reactions involving the above heterogeneous catalysts require longer time, higher temperature with moderate yield of the products. In case of the sulfuric acid absorbed on silica, the leaching of sulfuric acid and subsequent recyclability of the catalyst is a concern. Considering the above factors into account, we embarked upon the application of $MoO_3$-$ZrO_2$ materials as an environmentally benign and recyclable heterogeneous catalyst for synthesis of structurally diverse β-acetamido ketones.

The synthesis of β- acetamido ketones was carried out using $MoO_3$(20%)-$ZrO_2$ catalysts by one pot condensation of aryl aldehydes, enolizable ketones, and acetyl chlorides in acetonitrile (Scheme 1).

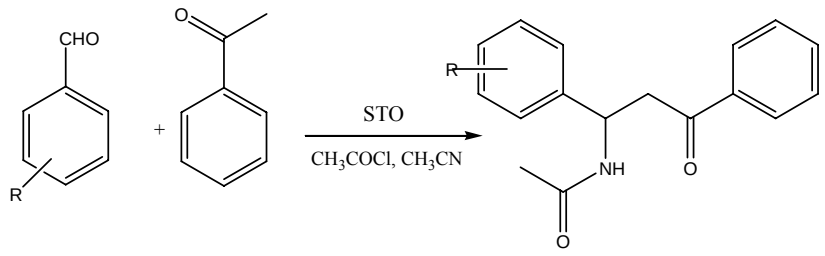


**(Scheme 1)**

Initially, the reaction conditions were optimized by varying different catalyst amount, stoichiometry of the reactants and reaction temperature. The preferred ratio of aryl aldehyde, ketone, and acetyl chloride was found to be 1:1: 2 using acetonitrile as a solvent as well as reactant. It was observed that, for a reaction involving 2 mmol of the aldehyde, 100 mg of the catalyst ideally suited for the efficient room temperature four component conversion and further increase in the catalyst amount does not significantly improve the conversion (Table 1). Similarly, the optimum temperature for the catalytic condensation was found to be 50$^{o}$C. The generality of the protocol was verified by introducing different structural variation in the aryl aldehyde (Table 1). The catalyst was found to be highly active for the different substituted benzaldehydes. The used 20MoZr catalyst after filtration and drying was reactivated by heat treatment at 400$^{o}$C for 1 h in air. The regenerated catalyst was used for two consecutive cycles without significantly losing its activity (Table 1, Entry 4, yields, 85%, 1st; 80%, 2$^{nd}$).

**Table 1. $MoO_3$(20%)-$ZrO_2$ catalyzed synthesis of β- acetamido ketones by one pot condensation of aryl aldehydes, enolizable ketones, and acetyl chlorides in acetonitrile.**

| Sl. No | R | Product | Time (h) | Yield (%) | MP | MP* |
|---|---|---|---|---|---|---|
| 1 | H | 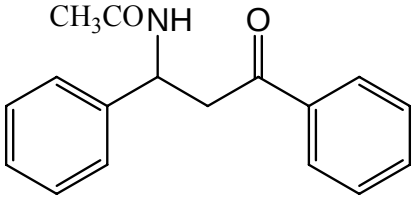 | 5 | 68 | 102 | 103 |
| 2 | 4-Cl | 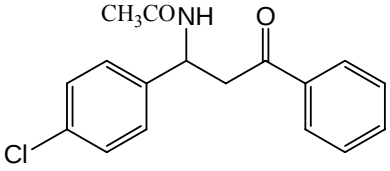 | 5 | 78 | 145 | 145 |
| 3 | 2-Cl | 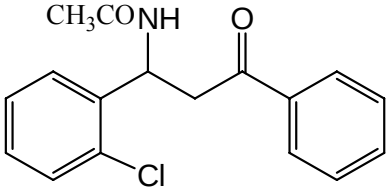 | 5 | 73 | 135 | 136-137 |
| 4 | 4-$NO_2$ | 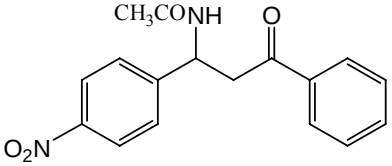 | 4 | 85 | 151 | 150 |
| 5 | 3-$NO_2$ | 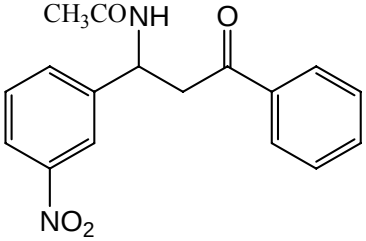 | 4 | 82 | 141 | 141-143 |

*Literature reported (Ref.. 30-33)

Mechanistically, the activated arylaldehyde initially acylated to the intermediate **I** which upon reaction with the enolic form of acetophenonne and after proton exchange gives **II**. Next, acetonitrile, attack **II** with the elimination of acetate group to give **III**. Hydrolysis of **III** followed by tautomerization gives the desired β- Acetamido ketones.

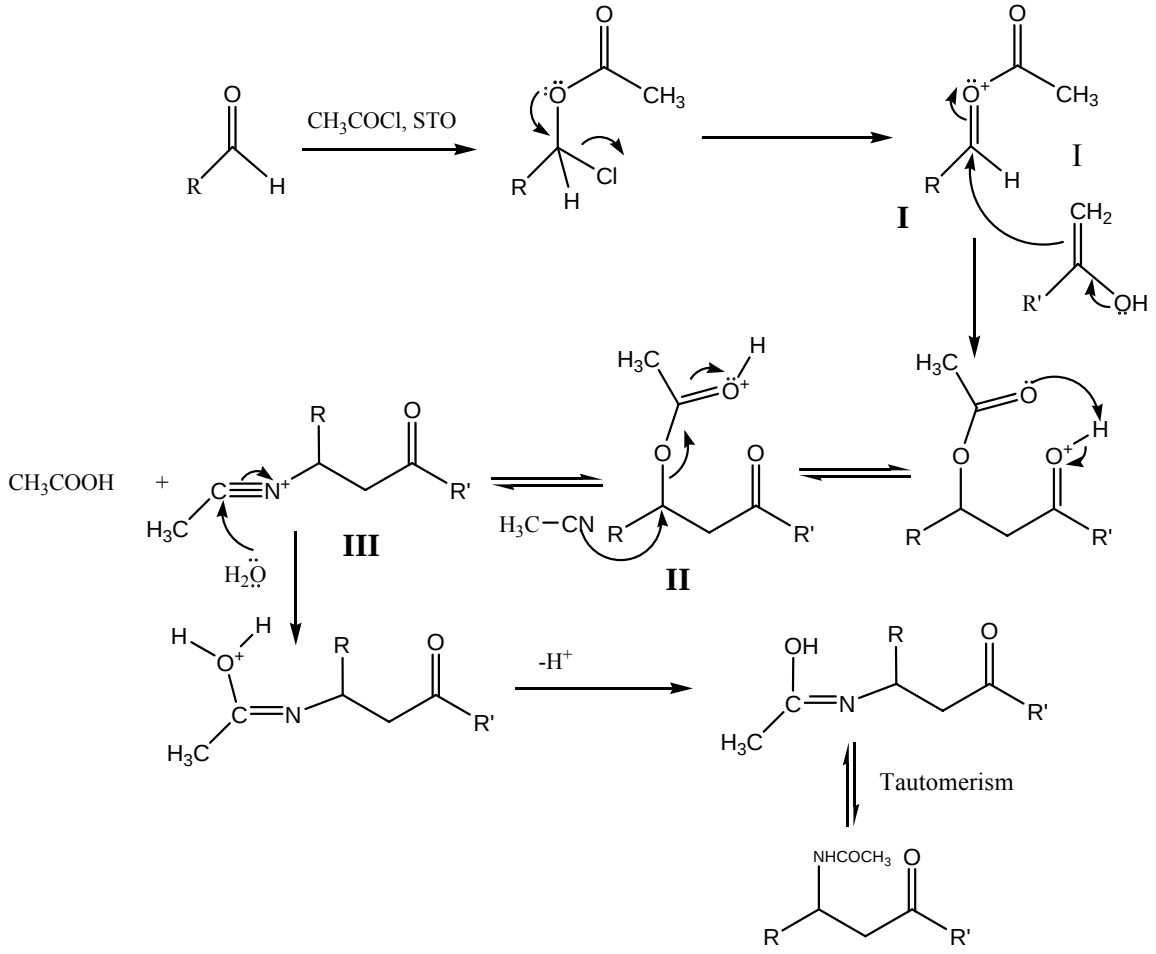


**(Scheme 2)**

The 20MoZr catalyst can help in more than one step in the mechanism in expediting the synthesis of β- Acetamido ketones. The aldehydic carbonyl group can be activated by adsorption onto the Lewis acidic sites of catalyst. Similarly, the process of enolization of the acetophenone can be catalyzed in the presence of the Bronsted acidic sites of the 20MoZr catalyst. Finally, the hydrolysis of the intermediate **III** and the final tautomerism steps can also be catalyzed by the Bronsted acidic sites on the 20MoZr catalyst surface.

## 4. CONCLUSION

In this research report, we have described the synthesis, characterization and catalytic application of $MoO_3$(x mol%)-$ZrO_2$ catalyst with different composition. The $MoO_3$(x mol%)-$ZrO_2$ catalyst were prepared by pH controlled hydrolysis of the corresponding salt precursors. For the sake of comparison the catalyst was also prepared by conventional wet impregnation technique. It was observed by XRD that the method of preparation plays an important role in controlling the phase transformation of the $ZrO_2$. In the former preparation case, the tetragonal phase was found to be selectively stabilized in presence of Mo. The martensitic phase transformation of the monoclinic to tetragonal phase was accomplished at much lower temperature in presence of $MoO_3$ in $ZrO_2$ matrix. The particle size calculated using Scherrer's equation was found to be in the range of 10-20 nm. Raman study conducted on the sample indicates the presence of various molecular species and clusters of $MoO_3$ on the surface of the $ZrO_2$. At least three type of molecular species such as $MoO4^{2-}$, $Mo_7O_{24}^{6-}$ and $Mo_8O_{26}^{6-}$ was observed on the surface of zirconia. The $MoO_3$(x mol%)-$ZrO_2$ materials were used as a efficient catalyst for the multicomponent condensation of aryl aldehydes, aryl ketones, acetic chloride and acetonitrile to yield the β-acetamidoketones. The protocol developed in the study is advantageous in terms of recyclable catalyst, simple, high yielding, devoid of toxic chemicals and high purity of the products.

## REFERENCES


[1] R.L. Augustine, Heterogeneous catalysis for the synthetic chemist. Marcel Dekker Inc., New York, 1996.

[2] T. Seiyama, *Catalysis Review Science and Engineering*, 34 (1992) 281.

[3] G.K. Boreskov, *Kinetics and Catalysis*, 14 (1973) 7.

[4] M.A., Aramendia, V. Borau, C. Jimenez, J.M. Marinas and F.J. Urbano, *Chemistry Letters* (1994) 1361.

[5] R. Pitchai, and K. Klier, *Catalysis Review Science and Engineering*, 28 (1986) 13.

[6] A. Corma, *Chemical Reviews*, 95 (1995) 559.

[7] P. D. L. Mercera, J. G. Van Ommen, E. B. M. Doesburg, A. J. Burggraaf and J. R. H. Ross, *Applied Catalysis* 57 (1990) 127.

[8] H. Hattori, *Chemical Reviews* 95 (1995) 537

[9] X. Song and A. Sayari, *Catalysis Reviews Science & Engineering* 38 (1996) 329

[10] G. Ranga Rao, *Bulletin of Material Sci.* 22 (1999) 89.

[11] W. Stichert, F. Schuth, *Chemistry of Materials* 10 (1998) 2020.

[12] M. H. Bocanegra-Bernal, S. D´iaz de la Torre, *Journal of Material Science* 37 (2002) 4947.

[13] M. Shelef, and R.W. McCabe, *Catalysis Today* 62 (2000) 35.

[14] M. Mogensen, N.M. Sammes and G.A. Tompsett, *Solid State Ionics*, 129 (2000) 3.

[15] J. Kašpar, P. Fornasiero and N. Hickey, *Catalysis Today* 77 (2003) 419.

[16] G. Ranga Rao, J. Kašpar, S. Meriani, R.D. Monte and M. Graziani, *Catalysis Letters* 24 (1994) 107.

[17] A. Trovarelli, C. de Leitenburg, M. Boaro and G. Dolcetti (1999) *Catalysis Today* 50, 353-367.

[18] W. Zhou, R. Ran, Z. Shao, *Journal of Power Sources* (2009) (available on line)

[19] S.P.S. Badwal, K. Foger, *Ceramic International* 22 (1996) 257.

[20] Nicholas C. P.; Marks T. J. *Nano Letters 4* (2004) 1557

[21] K.Arata, M.Hino, *Applied Catalysis 59* (1990) 197.

[22] A.Clearfield, G.P.D. Serrete, A.H. Khazi-Syed, *Catalysis Today 20* (1994) 295.

[23] H. Armenda´riz, M. A. Cortes, I. Herna´ndez, J. Navarrete, A. Va´zquez, *Journal of Material Chemistry* 13 (2003) 143.

[25] D. G. Barton, M. Shtein, R. D. Wilson, S. L. Soled, E. Iglesia, J. Phys. Chem. B 103 (1999) 630.

[26] C. D. Baertsch, S. L. Soled, E. Iglesia, J. Phys. Chem. B 105 (2001) 1320.

[27] B.M. Devassy, F. Lefebvre, S.B. Halligudi, J. Catal. 231 (2005) 1.

[28] K. V.R. Chary, K. R. Reddy, G. Kishan, J.W. Niemantsverdriet, G. Mestl, Journal of Catalysis 226 (2004) 283.

[29] T. Bhaskar, K. R. Reddy, C. P. Kumar, M. R.V.S. Murthy, K. V.R. Chary, Applied Catalysis A: General 211 (2001) 189–201

[30] U. Dahn, H. Hagenmaier, H. Hohne, W. A. Konig, G. Wolf, H. Zahner, Arch. Microbiol. 107 (1976) 249.

[31] H. D. Dakin, R. West, J. Biol. Chem. 78 (1928) 745.

[32] (a) M. Mukhopadhyay, B. Bhatia, J. lqbal, Tetrahedron Letts. 38 (1997) 1083; (b) G. Pandey, R. P. Singh, A. Garg, V. K. Singh, Tetrahedron Letters 46 (2005) 2137;

(c) R. Ghosh, S. Maity, A. Chakraborty, Synlett (2005) 115; (d) R. Ghosh, S. Maity, A. Chakraborty, S. Chakraborty, A.K. Mukherjee, Tetrahedron 62 (2006) 4059.

[33] (a) D. Bahulayan, S. Das, J. Iqbal, J. Org. Chem. 68 (2003) 5735; (b) T. Yakaiah, G. Reddy, B.P. Lingaiah, B. Narsaiah, P.S. Rao, Synth. Commun. 2005, 35, 1307; (c) M. T. Maghsoodlou, A. Hassankhani, H. R. Shaterian, S. Mostafa and E. Mosaddegh, Tetrahedron Letts. 48 (2007) 1729.